AD-A106 416 BOSTON COLL CHESTNUT HILL MA DEPT OF PHYSICS F/G 3/2
PREDICTING PROTON EVENT TIME CHARACTERISTICS FROM RADIO BURST D--ETC(U)
JUN 81 P BAKSHI, T NGUYEN F19628-79-C-0084
UNCLASSIFIED SCIENTIFIC-1 AFGL-TR-81-0185 NL

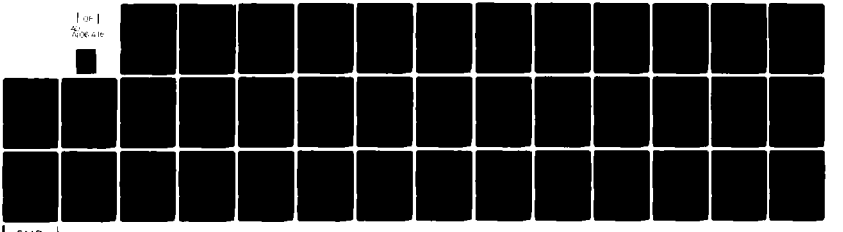

END
DATE FILED
11-81
DTIC

(18) (19) AFGL-TR-81-0185

LEVEL II (12)

(16) PREDICTING PROTON EVENT TIME CHARACTERISTICS FROM RADIO BURST DATA

AD A106417

(10) Pradip Bakshi
Thao Nguyen

Boston College
Department of Physics
Chestnut Hill, Massachusetts 02167

(11) Jun[redacted]81 (12) 39

(14) Scientific [redacted]-1

(15) F19628-79-C-0084 (16) 4643 (17) 03

AIR FORCE GEOPHYSICS LABORATORY
AIR FORCE SYSTEMS COMMAND
UNITED STATES AIR FORCE
HANSCOM AFB, MASSACHUSETTS 01731

unclassified

SECURITY CLASSIFICATION OF THIS PAGE (When Data Entered)

REPORT DOCUMENTATION PAGE		READ INSTRUCTIONS BEFORE COMPLETING FORM
1. REPORT NUMBER AFGL-TR-81-0185	2. GOVT ACCESSION NO.	3. RECIPIENT'S CATALOG NUMBER
4. TITLE (and Subtitle) Predicting Proton Event Time Characteristics from Radio Burst Data		5. TYPE OF REPORT & PERIOD COVERED Scientific Report No. 1 6. PERFORMING ORG. REPORT NUMBER
7. AUTHOR(s) Pradip Bakshi Thao Nguyen		8. CONTRACT OR GRANT NUMBER(s) F 19628-79C-0084
9. PERFORMING ORGANIZATION NAME AND ADDRESS Department of Physics Boston College Chestnut Hill, Mass. 02167		10. PROGRAM ELEMENT, PROJECT, TASK AREA & WORK UNIT NUMBERS 62101 F 464303 AX
11. CONTROLLING OFFICE NAME AND ADDRESS Air Force Geophysics Laboratory Hanscom AFB, Mass. 01731 Contract Monitor - W.R. Barron/PHP		12. REPORT DATE June, 1981 13. NUMBER OF PAGES 39
14. MONITORING AGENCY NAME & ADDRESS(if different from Controlling Office)		15. SECURITY CLASS. (of this report) Unclassified 15a. DECLASSIFICATION/DOWNGRADING SCHEDULE

16. DISTRIBUTION STATEMENT (of this Report)

Approved for public release, distribution unlimited.

17. DISTRIBUTION STATEMENT (of the abstract entered in Block 20, if different from Report)

18. SUPPLEMENTARY NOTES

19. KEY WORDS (Continue on reverse side if necessary and identify by block number)

Solar Protons
Solar Radio Bursts
Correlations, Solar Protons vs. Radio Bursts
Predicting Solar Proton Onset Time
Predicting Solar Proton Peak Flux Time
Solar Proton Time Characteristics

20. ABSTRACT (Continue on reverse side if necessary and identify by block number)

For events originating on the Western hemisphere, the delay before onset of the solar flare protons is shown to be well correlated ($r \sim 0.80$) with the rise time of the associated radio-burst at 2-3 GHz or the rise time of the H_α flare. The peak flux time of the protons is shown to be very well correlated ($r \sim 0.90$) with the delay before onset, and fairly well correlated ($r \sim 0.70$) with the flare or radio rise time. These results allow a prediction of the proton event time characteristics from real time radio burst data.

DD FORM 1 JAN 73 1473 EDITION OF 1 NOV 65 IS OBSOLETE

SECURITY CLASSIFICATION OF THIS PAGE (When Data Entered)

I. INTRODUCTION

The importance of solar flare radio spectra as predictors of significant proton events is widely recognized by now. The original studies[1-3] dealt with the basic yes-no criterion (U shaped radio-spectrum). Subsequently the question of predicting the magnitudes of the proton events was tackled using various measures of the radio spectrum, such as the time integrated flux-density at a given frequency,[4,5] peak flux-density, mean flux-density and duration,[5] or flash phase integrated flux-density.[6] The next significant development was the recognition[7-9] that even the slope of the proton peak flux profile could be predicted by using certain characteristics (essentially the width) of the U-spectrum. Recently, an improved technique for the prediction of the proton peak flux magnitudes has been developed,[10-12] (i) which restricts the time integration of the radio flux at a given frequency to the duration of the U, (ii) which uses the radio energy obtained by integration over a frequency range as the correlate, and (iii) which incorporates a heliographic longitudinal correction based on the location of the flare. On the basis of these studies, it is now possible to predict the proton peak flux spectrum from real time radio burst data.

One important question, however, still remains unanswered: When will these protons begin to arrive? When will they reach their peak flux values? More generally, what can be said about their time development? It is this broad area that we discuss in this report, and in particular, we determine some correlates from the radio data that would serve, for a given event, as predictors for the corresponding proton time characteristics.

The time development of the proton fluxes can be understood in terms of the following three parameters: (i) T_1, the delay before onset, or the time

interval between the peak of the radio flux and the time at which the proton flux (at a given energy) shows a sudden increase; (ii) T_M, the peak flux time, or the time interval between the peak of the radio flux and the peak of the proton flux (at a given energy); (iii) T_D, the decay time scale, (also at a given energy), which can only be described as an order of magnitude time scale in view of the difficulty of assigning a precise end-time to a given proton event. If the proton flux decays exponentially after reaching the peak, one can define the decay time scale to be the characteristic time appearing in the exponent. Many events, however, do not follow such a simple decay pattern and in several cases, new events start out before a significant decline has occurred from the peak of the preceding event. From the practical point of view, one is more interested in the time of onset T_I and the peak time T_M, -- these are the primary items to be predicted on the basis of the radio data.

It has been known for some time that the Eastern hemispheric events generally have larger onset and peak times than the Western hemispheric events, and that this can be understood[13] in terms of the much larger propagation time to reach the "foot-point" through the solar atmosphere for the protons from Eastern events. We have studied the particle events for 1967-69 by dividing the visible hemisphere into six equal (30^o) intervals and confirmed the earlier findings that the three Eastern sectors produce large onset and peak times compared to the three Western sectors, which typically have particle onset times of less than an hour. This is true irrespective of which energy channels are used for the particles. We also found that within the three Western sectors, there was no significant difference between the average arrival times of the particles. The

considerable spread that still exists for the individual arrival times of the Western hemispheric events must then be understood in terms of other parameters and effects.

In this Report we demonstrate that one such parameter, which seems to have a good correlation with the proton onset time T_1, is the rise time ρ of the associated flare or radio burst. It is further shown that the proton onset time T_1 is well correlated with the proton peak time T_M. Finally, combining these results, the flare or radio rise time is shown to be well related to the proton peak time.

We confine our attention to the Western hemispheric events so as to eliminate the propagation delay factor, characteristic of the Eastern hemispheric events. For the proton data, we primarily use the $29<E<94$MeV channel for which 10 minute interval data are available. In view of the small values of the onset time, such accurracy in the raw data for protons is indispensable. The data selection and the correlations between T_1 and ρ are discussed in section II. Correlations between T_M and T_1, and T_M and ρ, are discussed in section III, followed by a discussion of the results in section IV.

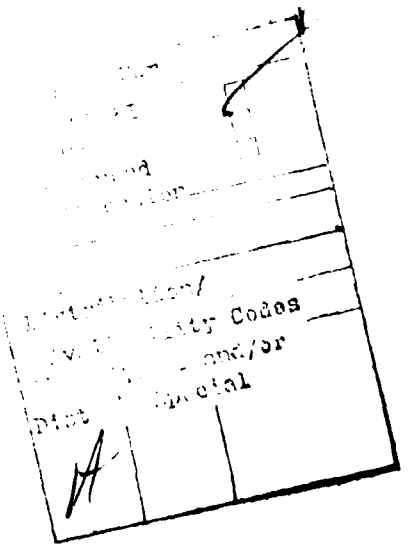

II. DELAY BEFORE ONSET

A. Data Base

As mentioned in the previous section, we restrict our attention to the Western hemisphere events. The raw data for 16 events during 1967-69 are presented in Table I. The original sources for the 29<E<94 MeV channel are the IMP4 data of Simpson and for the >30 MeV and >10 MeV channels are the IMP4 and IMP5 data of Bostrom, Williams and Arens, (see Ref. 14 for details). The primary focus is on the 10-minute averaged data in the 29≤E<94 MeV proton channel(designated in the tables simply as >29). These were obtained by detailed readings of the raw data compiled in digitized and semigraphic form on continuous computer print-outs (SSI) prepared by Smart and Shea. Information on other channels has also been included for the sake of comparison. The >30 MeV and >10 MeV proton channel data were obtained from another computer generated catalog (SSII) prepared by Smart and Shea, which, amongst other things, gives the time of onset and the time of peak for various particle channels. Some of these data can also be found in the Simon-Svestka catalog.[14] The information in the last column marked >10R is taken from Reinhard's thesis,[15] and refers to the >10 MeV proton data as assessed by Reinhard.

The detailed data in the 29<E<94 MeV channel (taken from SSI) are available only for the period 1967-69 (ending in early 1969) and this is the primary factor restricting the data base. There were, in all, 24 events where some rise above the background level (typically 0.02 unit, unit≡protons cm^{-2} sec^{-1} $ster^{-1}$) was discernible and with which a Western hemisphere flare could be associated. Out of these, 6 had peak fluxes $\leq$0.1 unit and were deemed to be too weak even for the study of the peak time T_M. One event had a peculiar proton time profile, consisting of a sharp peak, followed by a decline almost to the original background, all within an hour, followed by a major event with

TABLE I

Flare, Radio and Proton Data

Index	Date Location		H_α	2-3GHz	>29	>30	>10	>10R
1	28 May 67	S	0529	0529	0625	0625±10	0615±5	0625
		M	0543	0542	0930	1030 a	1030 a	1100
	W32 N28	I			29·7	26·9	115	115
2	17 Feb 68	S	0252	0251	0335	0350±30	0350±30	0400
		M	0254	0256	0535	0600 a	1000 b	1000
	W47 N17	I			0·55	0·41	1·91	2·29
3	09 Jun 68	S	0830	0839	0945	0945±15	0945±15	1000
		M	0854	0851	1405	1400 a	1400 a	1400
	W09 S14	I			12·5	12·4	75	75
4	29 Sep 68	S	1617	1616	1715	1720 d	1720	1715
		M	1623	1621	2045	2100 a	2300 a	2300
	W51 N17	I			15	19	32	32
5	03 Oct 68	S	2343	2343	0105	0120±20	0120	0130
		M	0008	0020	0515	0500 a	0800 a	0800
	W36 S17	I			8·6	6·3	36	36·5
6	31 Oct 68	S	2340	2340	0155	0200 c	0130±30	0200
		M	0012	0011	1405	1500 a	1500 a	1500
	W37 S14	I			17	10·2	133	133
7	04 Nov 68	S	0524	0513	0605	0600±10	0600±10	0615
		M	0529	0523	0815	0800 a	0800 a	0900
	W90 S15	I			8·75	4·9	19·3	19·6
8	18 Nov 68	S	1026	1026	1055	e	e	1115
		M	1035	1030	1315	1400 a	1400 a	1400
	W87 N21	I			467	403	849	849
9	24 Jan 69	S	0706	0705	0815	0830±40	0800±10	0830
		M	0728	0721	1305	1100 a	1230	1400
	W08 N20	I			0·7	0·15	3·2	3·47
10	25 Feb 69	S	0900	0905	0935	0930±10	0930±10	0945
		M	0913	0912	1155	1200	1300 a	1300
	W37 N13	I			33	30·5	88·4	88·7
11	27 Feb 69	S	1348	1400	1505	1500±20	1500±10	1500
		M	1413	1408	2145	2100 b	2200 a	2200
	W65 N12	I			12·5	9·3	28·1	28·4
12	14 Aug 68	S	1327	1326	-	-	-	-
		M	1332	1339	1755	1900 a	2000 a	2000
	W80 N13	I			0·2	e	0·69	0·95

TABLE I (continued)

Flare, Radio and Proton Data

Index	Date Location		H_α	2-3GHz	>29	>30	>10	>10R
13	30 Oct 68	S	1235	1235	-	-	-	-
		M	1252	1250	1445	1500 a	1500 a	1500
	W25 S18	I			0·19	0·11	1·02	1·45
14	24 Feb 69	S	2305	2307	-	-	-	-
		M	2313	2314	0125	-	0200 a	0200
	W31 N12	I			0·16	e	0·3	0·63
15	26 Feb 69	S	0418	0416	-	-	-	-
		M	0427	0425	0835	0900 a	0900 a	1200
	W46 N21	I			7·2	5·2	14·4	14·7
16	12 Mar 69	S	1739	1738	-	-	-	-
		M	1742	1740	2105	2100 a	2100 a	2100
	W80 N12	I			1·21	0·83	2·18	2·51

a: Time accurate to within one hour.

b: Time uncertainty greater than one hour.

c: Start superimposed on previous event.

d: Estimate because of missing data.

e: Missing data.

S: Start time.

M: Time of Maximum.

I: Proton Flux in cm^{-2} sec^{-1} $ster^{-1}$.

a slow decline. It was impossible to decide which proton peak should be associated with the radio or optical flare. Of the remaining 17 events, 11 listed chronologically as nos. 1-11 in Table I had a clear onset time. Nos. 12-14 were too weak to provide a reliable onset time, but strong enough to be considered for studying T_M. No. 15 was superimposed on a very high tail from the preceding event, and thus could not be used for the study of T_1. No. 16 had a small precursor before the main event in its proton profile. Its onset time could not be determined, since the precursor was well above the background. One more event (not listed) also had a similar problem, perhaps a bit more pronounced. Again it was not clear whether to treat that as a double proton event (in which case even the T_M remains in doubt), or as a single event where at least the T_M information is reliable for correlations. Thus, we are left with 16 events, of which nos. 12-16 could be used for the study of T_M, but not of T_1.

The H_α-flare and 2-3GHz radio burst data were generally obtained from the Simon and Svestka catalog.[14] In some cases, where detailed radio burst time profiles were available (as in Barron et al.[16]) it was possible to refine the radio information. We had also used the catalogs of Castelli and Barron[17] and Castelli and Tarnstrom,[18] where applicable.

B. Correlations

The data in Table I provide the start-time (S) and maximum-time (M) for the flare (H_α), the radio-burst (in 2-3 GHz range) and the four proton channels. The 29<E<94 MeV channel is simply referred to as >29 for convenience. From these raw data, one can calculate various time intervals such as the delay before onset T_1 for a particular energy channel, measured from the peak-time of the flare or of the radio burst. One can also use the start-time of the

flare (or the radio-burst) as the reference time in measuring the delay before onset. We designate this as T_{1S}. For any given proton channel we have four possible choices to measure the "delay before onset": $T_1(H_\alpha)$, T_1(2-3GHz), $T_{1S}(H_\alpha)$ and T_{1S}(2-3GHz).

Empirically, one can argue that something unusual starts happening on the sun when the H_α flare starts or when the radio burst starts. Usually, the two start times are coincident or within one or two minutes of each other. Of the sixteen events listed in Table I, twelve are in this category. We prefer to measure <u>all</u> times from the <u>start</u> of the flare or from the <u>start</u> of the radio burst. While studying correlations with radio parameters, we will use the start of the radio-burst as the reference point. Thus, the radio rise time ρ(2-3GHz) will be considered in relation to T_{1S}(2-3GHz). Similarly, the flare rise time $\rho(H_\alpha)$ will be considered in relation T_{1S} (H_α). Using T_1 instead of T_{1S} presupposes that nothing of importance occurs <u>prior</u> to the peak of the radio-burst or the peak of the flare. This certainly would not be true for events with long rise times for H_α or the radio-burst. In fact, in some cases the H_α or radio rise times ρ reach almost a third of the proton delay before onset T_{1S}. We thus consider the direct empirical variable T_{1S} to be the more basic, and the subsequent analysis in this section deals with the correlations between T_{1S} and ρ.

Table II provides the rise times ρ, designated by H for H_α and G for 2-3GHz, in the third column. The delays before onset T_{1S} for each of the four proton channels (with the H_α or the radio start time as the reference) are given in the next four columns. The last four columns provide T_{MS}, the peak flux times of the proton event in the four channels as measured from the start of the H_α

TABLE II

Flare(H), Radio(G), and Proton Time Intervals

(in minutes)

Index			T_{1S}				TMS			
		ρ	>29	>30	>10	>10R	>29	>30	>10	>10R
1	H	14	56	56	46	56	241	301	301	331
	G	13	56	56	46	56	241	301	301	331
2	H	2	43	58	58	68	163	188	428	428
	G	5	44	59	59	69	164	189	429	429
3	H	24	75	75	75	90	335	330	330	330
	G	12	66	66	66	81	326	321	321	321
4	H	6	58	63	63	58	268	283	403	403
	G	5	59	64	64	59	269	284	404	404
5	H	25	82	97	97	107	332	317	497	497
	G	37	82	97	97	107	332	317	497	497
6	H	32	135	140	110	140	865	920	920	920
	G	31	135	140	110	140	865	920	920	920
7	H	5	41	36	36	51	166	156	156	216
	G	10	52	47	47	62	177	167	167	227
8	H	9	29	-	-	49	179	214	214	214
	G	4	29	-	-	49	179	214	214	214
9	H	22	69	84	54	84	359	234	324	484
	G	16	70	85	57	85	360	235	325	485
10	H	13	35	30	30	45	175	180	240	240
	G	7	30	25	25	40	170	175	235	235
11	H	25	77	72	72	72	477	432	492	492
	G	8	65	60	60	60	465	420	480	480
12	H	5	-	-	-	-	268	333	393	393
	G	13	-	-	-	-	269	334	394	394
13	H	17	-	-	-	-	130	145	145	145
	G	15	-	-	-	-	130	145	145	145
14	H	8	-	-	-	-	140	-	175	175
	G	7	-	-	-	-	138	-	173	173
15	H	9	-	-	-	-	257	282	282	462
	G	9	-	-	-	-	259	284	284	464
16	H	3	-	-	-	-	206	201	201	201
	G	2	-	-	-	-	207	202	202	202

flare or the radio-burst.

Figure 1 is a graph of T_{1S} vs $\rho(H_\alpha)$ for the >29 channel protons for eleven events, nos. 1-11. Larger rise times seem to be associated with larger delays before onset. Using a best-fit straight line $y=a+bx$, with $y=T_{1S}$ and $x=\rho$, we find a correlation coefficient $r=0.839$ and a standard deviation $\sigma=15.4$ minutes. The best fit line is represented by the solid line, with $a=23.5$ minutes and slope $b=2.496$.

The corresponding results based on 2-3 GHz radio data are presented in Figure 2, with $r=0.787$, $\sigma=17.1$ minutes, $a=34.4$ mins and $b=2.093$. Both Figures 1 and 2 show a clear trend, with T_{1S} increasing with increasing ρ. The correlation coefficients and the standard deviations are not significantly different in the two cases. The differences in a and b stem from the unusually large rise time (37 min) for the radio-burst for event no. 5.[19]

We have evaluated the correlations for all the proton energy channels listed in Table II, obtaining the results presented in Table III, lines 1-12. The >30 and >10 channels have only 10 events as event no. 8 could not be included due to missing data. The other two channels have also been considered with the same 10 events to obtain a uniform comparison. These results show that the correlation coefficient r ranges from 0.76 to 0.86, with the exception of line 7. The standard deviation σ remains around 15 minutes in all cases.

We can now draw some inferences. (1) From lines 1-4 we see that there is no significant difference between H_α and 2-3GHz data in terms of r or σ. We had also considered 200-600 MHz radio data for comparison, but the correlations were slightly poorer. (2) Even though the >29 channel proton data have a finer resolution, the other channels provide comparable results. This may be accidentally so, due to the small data base. One would have expected to see larger standard deviations in the other channels. (3) There is a slight increase

TABLE III

Correlations: T_{1S} vs ρ

Proton Channel	No. of Events	Predictor	r	σ min.	a min.	b	line	Remarks
>29	n=11	H	0·839	15·4	23·5	2·496	1	Fig. 1
		G	0·787	17·1	34·3	2·093	2	Fig. 2
	n=10	H	0·835	15·1	27·5	2·356	3	
		G	0·765	17·3	37·7	1·961	4	
>30	n=10	H	0·776	18·9	30·8	2·396	5	
		G	0·799	17·9	37·0	2·282	6	
>10	n=10	H	0·716	16·8	34·3	1·776	7	
		G	0·804	13·8	37·2	1·796	8	Fig. 3
>10R	n=11	H	0·800	16·6	37·1	2·325	9	
		G	0·861	14·0	42·8	2·278	10	
	n=10	H	0·787	17·1	39·3	2·250	11	
		G	0·849	14·6	43·4	2·250	12	
>30	n=14	G	0·674	22·6	38·0	2·183	13	
>10	n=14	G	0·650	17·5	40·7	1·585	14	Fig. 4
>10R	n=15	G	0·728	17·2	48·6	1·947	15	

in the intercept a of the >10 or >10R MeV channels compared to the >29 or >30 MeV channels. This is an indication of velocity dispersion; the higher energy particles can be expected to have smaller delays before onset. (4) The systematic difference between the >10 channel (lines 7,8) and the >10R channel (lines 11,12) shows the sensitivity of the correlations to the subjective reading of the same data by two observers in judging the onset times.

C. Additional Data

With the observation that the other energy channels provide comparable correlations, we can now extend the data base beyond the termination time of the >29 channel. Criteria similar to the ones used in screening the events of Table I lead to 5 additional events for the period through 1973. Several events were eliminated as the uncertainty in their onset-time was of the order of one hour. These 5 additional events are listed in Table IV in a format similar to Table I, except for the omission of the >29 column. Since our primary interest is in developing radio-burst proton correlations, only the radio rise time information is given in Table IV. The ensuing radio and proton time intervals are given in Table V. Only 4 events, nos. 17-20 can be used for T_{IS} studies, since no. 21 is too weak to provide a reliable onset time. There is considerable discrepancy in the peak times reported in different channels for event nos. 17-20. It is quite likely that these are multiple peak events, and consequently, we have given a single column for T_{MS} in Table V, based on the earliest of these multiple peaks. In the case of event no. 20, the >60 MeV channel, not mentioned in Table IV, had a peak at 0200, and the corresponding interval is given as T_{MS} in Table V. For the other three events (Nos. 17-19) the >60 MeV peak was quite close to the corresponding >30 MeV peak.

TABLE IV

Radio and Proton Data

Index	Date Location		2-3GHz	>30	>10	>10R
17	29 Mar 70	S	0037	0130±10	0140±10	0200
		M	0040	1900 a	1900 a	0800
	W37 N17	I		20	65	44
18	24 Jan 71	S	2310	2336±10	2336±10	0000
		M	2323	0700 b	1300 b	1300
	W49 N18	I		407	1170	1171
19	06 Apr 71	S	0936	1120±20	1100±30	1030
		M	0946	1600 a	1720 a	1800
	W80 S19	I		5	50.5	51.4
20	01 Sep 71	S	1934	2010±10	2020±20	2100
		M	1941	0730 a	0730 a	0800
	W120 S10	I		162	352	352
21	02 Dec 71	S	0102	-	-	-
		M	0120	-	0700 a	0700
	W66 S15	I			1	1.54

a: Time accurate to within one hour.

b: Time uncertainty greater than one hour.

S: Start time.

M: Time of Maximum.

I: Proton Flux in cm^{-2} sec^{-1} $ster^{-1}$.

TABLE V

Radio and Proton Time Intervals
(in minutes)

Index	ρ	T_{1S} >30	T_{1S} >10	T_{1S} >10R	T_{MS}
17	3	53	63	83	443
18	13	26	26	50	470
19	10	104	84	54	384
20	7	36	46	86	386
21	18	-	-	-	358

The last three lines of Table III provide the correlations for T_{1S} vs. ρ when these four additional events (nos, 17-20) have been added to the earlier sets. For > 30 MeV, r declines from 0.799 (n=10) to 0.674 (n=14) and σ increases from 17.9 min. to 22.6 min. The character of the best fit line remains unaltered as changes in a and b are negligible. There are similar results for the >10 and >10R channels. The changes are graphically illustrated in Figures 3 and 4 for the >10MeV channel. Figure 3, based on only the cleaner data of 1967-69 has a smaller $\sigma \approx$ 13.8 mins. The standard deviation increases to 17.5 mins. in Figure 4, which includes the additional four events represented by solid triangles. This increase in spread can be ascribed to the slightly reduced accuracy of the observed onset times for the additional events.

The analysis of this section shows that there is a good correlation between the rise time of the flare or the radio-burst and the delay before onset of the protons in any channel. The remaining spread is to be expected, since there are probably many other factors which are related to the delay time. We will return to these questions in Section IV after developing the correlations for the peak time T_{MS} in the next section.

III. PEAK FLUX TIME

A. Data Base

The actual peak flux times of 16 events are listed for the various proton channels in Table I. The peak flux time intervals T_{MS}, defined as the actual proton peak flux time minus the actual start time of the flare (or the radio-burst) are listed in the last four columns of Table II.

The actual peak flux times for the >29 channel were determined by detailed readings of the 10 minute averaged data base (SSI). For event no. 1, the 10 minute peak occurred about an hour earlier than the peak for the hourly averaged data in the same channel. For event nos. 7 and 13, there were two peaks of almost equal fluxes, separated by 30 min. and 90 min. respectively. In both cases, the peak time entered in Table I was the average of the two observed peak times. For event no. 3, there were two peaks separated by 12 hours. We have recorded the first peak, which is synchronous with the >60 and >30 MeV channel peaks. The second peak was slightly higher, but the intervening (slight) decline suggests that there were two superposed events. A similar situation prevails for the >10 MeV channel as well, where the ultimate peak was 16 hours later, and had a much higher peak flux level. For event no. 11, there were two peaks, separated by three hours, the later peak was higher. The first peak was coincident with the >60 MeV peak, while the second was coincident with the >94, >30, and >10 MeV peaks. We have chosen the second peak in this case.

In some events, as in the case of no. 11, the fast rise terminates with a minor peak and then the flux level continues to increase at a much slower pace to culminate in one or more higher peaks. If we had a much larger data base, it would have been useful to study separately the correlations of T_{FS},

the time to reach the first peak at the end of the fast rise interval. We have carried out such an analysis for the >29 channel and since the differences from using T_{MS} were not very significant, we have not extended that to all channels.

B. Correlations: T_{MS} vs T_{1S}

It was observed during the study of section II that events with large delays before onset seemed to have a large peak flux time as well. Figure 5 is a graph of T_{MS} vs T_{1S} for the >29 channel, using the 2-3GHz radio burst start time as the reference time. The trend is quite apparent. The correlations with $y=T_{MS}$, $x=T_{1S}$ and using the best fit straight line $y=a+bx$ lead to $r=0{\cdot}936$, $\sigma=68{\cdot}7$ min., $a=-90{\cdot}5$ min. and slope $b=6{\cdot}597$. If we use the H_α flare start as the reference time, the results are very similar; $r=0{\cdot}958$, $\sigma=56{\cdot}5$ min., $a=-99{\cdot}0$ min. and $b=6{\cdot}635$. These excellent correlations suggest that the time development of a proton event may be governed by a single time scale, characteristic of that event. Furthermore, this time scale can be predicted from the flare or radio rise time according to the results of section II.

The correlations for all the channels are given in Table VI. The >30 and >10 channels have only 10 events, since T_{1S} for event no. 8 is not available. The data for the >29 and >10R channels are given for the full set of events (n=11), and also for (n=10) corresponding to the other two channels. The data are less accurate in the other channels as compared to the 10 minute data of the >29 channel and this is reflected in the slightly lower correlations in the other channels. A typical case is shown in Figure 6, which represents graphically the events for the >10 MeV channel, using the 2-3 GHz radio burst start time as the reference time. The correlation coefficient is r=0.855 and the standard deviation rises to $\sigma=102.6$ min.

TABLE VI

Correlations: T_{MS} vs T_{1S}

Proton Channel	No. of Events	Reference Start Time	r	σ min.	a min.	b	line	Remarks
>29	n=11	H	0·958	56·5	-99·0	6·635	1	
		G	0·936	68·7	-90·5	6·597	2	Fig. 5
	n=10	H	0·965	52·6	-132·4	7·019	3	
		G	0·940	67·8	-120·5	6·948	4	
>30	n=10	H	0·856	110·2	-93·0	6·006	5	
		G	0·827	117·7	-73·6	5·815	6	
>10	n=10	H	0·870	98·2	-51·4	7·158	7	
		G	0·855	102·6	-49·6	7·243	8	Fig. 6
>10R	n=11	H	0·888	92·7	-41·5	6·091	9	
		G	0·873	92·4	-29·8	6·010	10	
	n=10	H	0·877	94·9	-25·1	5·935	11	
		G	0·861	95·3	-11·2	5·831	12	
>30	n=14	G	0·577	157·4	132·4	3·440	13	
>10	n=14	G	0·681	123·1	110·4	4·961	14	
>10R	n=15	G	0·799	98·1	40·1	5·193	15	

The following inferences can be drawn from Table VI: (1) There is little difference between using the H_α start time or the 2-3 GHz radio start time, although H_α results seem to be consistently better. (2) The >10 and >10R channels show an increase in σ from $\approx$ 60 min. of >29 channel to 90-100 min. The >30 channel shows a further increase to 110-120 min. This can be ascribed to the relative lack of precision in the determination of the proton start and peak times in these channels. (3) If we consider the additional four events beyond the time range of the >29 channel data, the results are given by the last three lines of Table VI. For >10 and >30 channels, the spread increases respectively to σ=123 and 157 min. The >10R channel results remain stable with no significant increase in σ, (98 min.). The correlations are not so good in the >30 (r=0·58) and >10 (r=0·68) channels, but remain reasonable (r=0·80) in the >10R channel.

C. Correlations: T_{MS} vs ρ

Combining the results above with those of section II, one can expect to find some correlation between the flare or radio rise time ρ and the proton peak time T_{MS}. Figures 7 and 8 describe graphically the correlations for the >29 channel, using H_α and 2-3GHz data respectively. For all the 16 events of Tables I and II, we find

H_α:	r=0·749	σ=115·7 min.	a=87·2 min.	b=14·46
2-3GHz:	r=0·605	σ=138·8 min.	a=145·7 min.	b=11·44

Here H_α is decidedly better than the radio correlation. Perusal of Figures 7 and 8 shows that the large radio rise time of 37 min. for event no. 5 is primarily responsible for this difference. This was a rather complex radio event, and a detailed analysis of the radio data time profiles (which are not easily available for this event) may reveal some special features.[19] Without this event, the H_α and radio results are comparable.

The corresponding numbers for the >10 channel (with 16 events) are,

H_α:	r=0·601	σ=147·5 min.	a=177·9 min	b=13·21
2-3GHz:	r=0·625	σ=143·7 min.	a=228·3 min	b=12·04

If we add to this all the five events of Tables IV and V, the correlations are slightly reduced, but σ improves due to the larger population (n=21),

2-3GHz: r=0·551 σ=137·1 min.

These results emphasize the need for data with high time resolution (such as the 10 minute averages of the >29 channel) and the need for a more detailed analysis when multiple peaks occur in proton profiles or when multiple peaks occur in the radio-burst profile.

IV. DISCUSSION

The previous two sections indicate that good correlations exist between the flare or radio-burst rise time ρ and the delay before onset T_{1S}, excellent correlations exist between T_{1S} and T_{MS} the proton flux peak time, and reasonably good correlations exist between ρ and T_{MS}. It became clear that the 10 minute averaged, directly read, >29 channel data provide the best results amongst the various proton channels. This is not surprising, since the time uncertainties in the reading of the other channels are generally much higher. In the data selection process, it was pointed out that the existence of multiple peaks in the proton profile creates ambiguities in the determination of T_{MS}. A less ambiguous question would be to study the time of the first peak, T_{FS}. This was examined for the >29 channel data and the correlations were comparable to the results for the strongest peak time T_{MS}. Besides these points, already mentioned in the previous sections, we now discuss a variety of other relevant topics.

1) Amongst proton channels, the >94 MeV and the >60 MeV channels did not register any noticeable increases in some of the events considered above. The total number of events in these channels was thus too small to be statistically significant, and these channels were not analyzed.

2) The radio-burst rise time was easily available for two frequency ranges from the Simon-Svestka catalog,[14] (2-3GHz and 200-600MHz). However, the start time was often later and the time of maximum often earlier in the latter range as compared to the former, resulting in generally smaller rise times ρ in the 200-600 MHz range. There was a noticeable clustering of events with rise times of 2 to 4 minutes, reducing significantly the

correlations in comparison with those based on the 2-3GHz range. The lower frequency range is thus not helpful for the prediction of proton time scales.

3) Even for the 2-3GHz and H_α data, it would have been very helpful if detailed time profiles had been available for each event. Such profiles were available in the radio band for a few of the events in the catalog of Barron et al.[16] and it was possible in the case of those events to check whether there were multiple radio peaks. We believe that a uniform review of the time profiles for all the events would have been useful, not only for directly ascertaining the precision of the reported[14] start and maximum times, but also in guarding against viewing a complex radio-burst as a single episode with a large rise time. Similar time histories of H_α profiles would also be useful for the same reasons.

4) The correlations between T_{1S} and ρ are quite good as shown in Table III and Figures 1-4. Can the spread around the best fit line be explained systematically in terms of other parameters? This question can be analyzed systematically by plotting the individual event deviations in T_{1S} from the best fit line against the parameter in question. It was found that the spread vs. longitude (west) was random for the H_α and also the 2-3GHz data. The spread vs. I_{29}, the proton peak flux in the $29<E<94$ channel, also does not show any trend. It is noteworthy, however, that the two strongest events have onset times almost a standard deviation ($\approx$15-20 mins.) earlier than that indicated by the best fit line. It would require a larger data base to ascertain whether this implies any systematic relation between the spread and high peak fluxes. Most of the events in Table I had a U-shaped radio-burst frequency spectrum. One was a weak-U (Event no. 2), two were flat (nos. 5 and 9), and one was a weak A (no. 12).[18] One (no. 13)

was not identified in terms of its radio signature in any of the catalogs. There was no specific pattern in terms of the spread in relation to the radio-burst signature. For a number of these events, the proton spectral slope β and the width[9] of the U, ω_3/ω_2, were available. There was no discernible pattern between the spread and β or the spread and (ω_3/ω_2). Again, it should be noted that one needs a larger data base to understand the spread in terms of other variables. All of the above factors were considered for T_{MS} vs ρ graphs as well and no specific explanation could be given for the spread in terms of these variables.

5) Reinhard and Wibberenz[13] analyzed the proton peak flux times in terms of $T_M=C_1+C_2/V$, where C_1 is a longitude dependent propagation time and C_2 is independent of the longitude. The second term represents the effect of velocity dispersion. We did not have enough events in the >94 MeV channel to determine the velocity dispersion in terms of the 10 minute averaged data. If we take the C_1 and C_2 for various events as given in Reinhard's thesis,[15] we can determine whether C_1 and C_2 individually show any correlation with ρ. We find no significant correlations between C_1 and ρ or C_2 and ρ, even though T_M and ρ have a fairly good correlation. This suggests that viewing T_M as a sum of a longitudinal factor and a velocity dispersion factor may not be a good model for the Western hemispheric events. Perhaps the uncertainties implicit in determining C_2 are too large to make C_1 and C_2 meaningful.

6) An important conclusion that emerges from the study of T_{MS} vs T_{1S} in section III is that each proton event seems to be governed by a single time scale, characteristic for that event. The time to reach the peak T_{MS} is proportional to the onset time T_{1S}. Furthermore, this characteristic time is

related to the rise time of the flare or the radio-burst. All this suggests that the entire process -- the flare, the radio burst, the proton profile, and possibly the other components of the flare phenomena -- is governed by a single time scale, characteristic of that event. If this is so, then empirically finding one aspect (e.g., the rise time ρ) allows one to infer the other aspects (e.g., T_{1S} or T_{MS}). From the theoretical point of view, any proposed model would have to explain the existence of such a single scale. In view of the importance of this question, it would be appropriate to extend this study to a larger data base with better resolution and also to examine whether the time scales for other concommitant processes such as x-ray bursts, electrons, etc. have similar correlations. We note that the decay time scale T_D, defined as the characteristic time in the exponent $\exp(-T/T_D)$ for the declining phase of the proton event, did not show any significant correlations to ρ, T_{1S} or T_{MS}.

7) An important distinction must be drawn between "correlations" and "predictions." Some correlation studies include selection criteria based on properties of the variable to be predicted. For example, 6 very weak events with peak flux $I_{29} \leq 0.1$ unit were excluded here at the outset. It would not be known from the rise time of H_α or of the 2-3 GH_z radio band whether the proton event is going to be a weak one. One has to rely on other studies[10-12] aimed at predicting the proton flux levels from radio data to determine whether it will be a weak event. If it is a weak event, a reliable prediction for its start time would not be possible on the basis of the correlations studied in this Report. Even for the range $0.1 \leq I_{29} \leq 0.2$, the 3 events in Table I in that range were found to be too weak to provide a reliable onset time (but not weak enough to be excluded for the

study of T_{MS}). So these correlations provide meaningful predictions for T_{1S} only for $I_{29} > 0.2$ unit and for T_{MS} only when $I_{29} > 0.1$ unit.

The use of the detailed characteristics of the proton time profile as a selection factor poses more serious problems from the point of view of predictions. We had also excluded at the outset two proton events on the basis of the occurrence of a strange precursor or small peak of short duration. The correlation study proceeded on the basis of excluding events where a clear identification between a proton peak and a flare or radio burst was not possible. It is not possible to predict from the flare or radio data whether the proton event will turn out to have a complex time profile of the type we have excluded. We will make a 'prediction' on the basis of these correlations, but if the actual event turns out to be a complex one, the prediction will not be valid. On the basis of this limited data base, after excluding weak events, the occurrence of complex events was 2 out of 18 for T_{MS} studies and 3 out of 14 for T_{1S} studies.

8) The results obtained in this Report suggest that further studies along these lines should be carried out over a wider data base. Other radio parameters such as the radio peak flux at a given frequency, time integrated radio flux at a given frequency, time and frequency integrated radio flux, the width of the U, and the detailed time development of the radio spectral shape can perhaps be used in conjunction with the simple rise time to improve the correlations and the predictions.

ACKNOWLEDGEMENT

We wish to thank D. Smart and M. Shea for providing the particle data base, and for many helpful discussions. We are much indebted to D. Guidice for his interest, support and suggestions. We also wish to thank E. Cliver and S. Kahler for many valuable comments. Continuous interaction with W. Barron has been indispensable; we are much indebted to him for his interest and many comments, and his willingness, always, to probe a little deeper for the radio data.

REFERENCES

1. Castelli, J.P., J. Aarons and G.A. Michael, Flux density measurements of radio bursts on proton-producing flares and nonproton flares, J. Geophys. Res., 72, 5491, 1967.

2. Castelli, J.P., Observations and forecasting of solar proton events, Report AFCRL-68-0104, Air Force Cambridge Research Laboratories, Hanscom AFB, MA, 1968.

3. Castelli, J.P., and J. Aarons, Radio burst spectra and the short term prediction of solar proton events, Proceedings of Symposium on Ionospheric Forecasting, Grey Rocks, Canada, 49, Paper No. 11, 1969.

4. Straka, R.M., and W.R. Barron, Multifrequency solar radio bursts as predictors for proton events, Proceedings of Symposium on Ionospheric Forecasting, Grey Rocks, Canada, 49, Paper No. 10, 1969.

5. Straka, R.M., The use of solar bursts as predictors of proton event magnitudes, AFCRL Space Forecasting Research Note, No. 2, Air Force Cambridge Research Laboratories, Hanscom AFB, MA, 1970.

6. Newell, D.T., Forecasting peak proton flux and PCA event magnitudes using flash-phase integrated radio-burst flux density, Report AFCRL-72-0543, Air Force Cambridge Research Laboratories, Hanscom AFB, MA, 1972.

7. Bakshi, P., and W. Barron, Spectral Correlations between solar flare radio bursts and associated proton fluxes, I, Report AFCRL-TR-74-0508, Air Force Cambridge Research Laboratories, Hanscom AFB, MA, 1974.

8. Bakshi, P., and W. Barron, Spectral Correlations between solar flare radio bursts and associated proton fluxes, II, Report AFCRL-TR-75-0579, Air Force Cambridge Research Laboratories, Hanscom AFB, MA, 1975.

9. Bakshi, P., and W. Barron, Prediction of Solar Flare Proton spectral slope from Radio Burst Data, J. Geophys. Res. 84, 131, 1979.

10. Bakshi, P., and W. Barron, Prediction of proton flux magnitudes from radio burst data, Report AFGL-TR-78-0100, Air Force Geophysics Laboratory, Hanscom AFB, MA, 1978.

11. Bakshi, P., and W. Barron, Prediction of Solar Flare Proton Spectrum from Radio Burst Characteristics, Solar Terrestrial Predictions Proceedings, Vol. 3, D7-D14, 1980, Ed. R. Donnelly, U.S. Govt. Printing office.

12. Barron, W., and P. Bakshi, Application of Integrated Radio Burst Fluxes to the Prediction of Solar Energetic Proton Flux Increases, Solar Terrestrial Predictions Proceedings, Vol. 3, D1-D6, 1980, Ed. R. Donnelly, U.S. Govt. Printing office.

13. Reinhard, R., and G. Wibberenz, Propagation of Flare Protons in the Solar Atmosphere, Solar Physics, 36, 473, 1974.

14. Svestka, Z. and P. Simon (Ed.), Catalog of Solar Particle Events 1955-1969, D. Reidel, Hingham, Mass., 1974.

15. Reinhard, R. Die Solare Ausbreitung Flareerzeugter Protonen Im Energiebereich 10-60 MeV, Ph.D. Thesis, Christian-Albrechts-Universität zu Kiel, kiel, 1975.

16. Barron, W., E. Cliver, D. Guidice and V. Badillo, An Atlas of Selected Multi-Frequency Radio Bursts From the Twentieth Solar Cycle, Report AFGL-TR-80-0098, Air Force Geophysics Laboratory, Hanscom AFB, MA, 1980.

17. Castelli, J., and W. Barron, A Catalog of Solar Radio Bursts 1966-76 having Spectral Characteristics predictive of Proton Activity, J. Geophys. Res. 82, 1275, 1977.

18. Castelli, J., and G. Tarnstrom, A. Catalog of Proton Events having Non-classical Solar Radio Burst Spectra, Report AFGL-TR-78-0121, Air Force Geophysics Laboratory, Hanscom AFB, MA, 1978.

19. A subsequent examination of various original sources for the radio-burst data for this event has revealed that the 37 minute rise time occurs at 3.75GHz, and not at 2.8GHz as reported in Reference 14. Other observatories provide a rise time of 16 minutes or 21 minutes in the 2-3 GHz band. With either of these figures, this event would move into the main population of events and the overall correlations would improve slightly. The H_α rise time for this event was 25 minutes and the 2-3 GHz results will be very similar to the H_α results if we use the smaller rise time. We are much indebted to W. Barron for the exhaustive search which brought out the various rise times from original sources.

FIGURE CAPTIONS

Figure 1. Delay before >29 MeV proton onset vs Rise time of the H_α flare.

Figure 2. Delay before >29 MeV proton onset vs Rise time in the 2-3 GHz radio frequency band.

Figure 3. Delay before >10 MeV proton onset vs Rise time of the H_α flare.

Figure 4. Delay before >10 MeV proton onset vs Rise time in the 2-3 GHz radio frequency band.

Figure 5. Time to reach peak for >29 MeV protons vs Delay before onset for the same channel.

Figure 6. Time to reach peak for >10 MeV proton vs Delay before onset for the same channel.

Figure 7. Time to reach peak for >29 MeV protons vs Rise time of the H_α flare.

Figure 8. Time to reach peak for >29 MeV protons vs Rise time in the 2-3GHz radio frequency band.

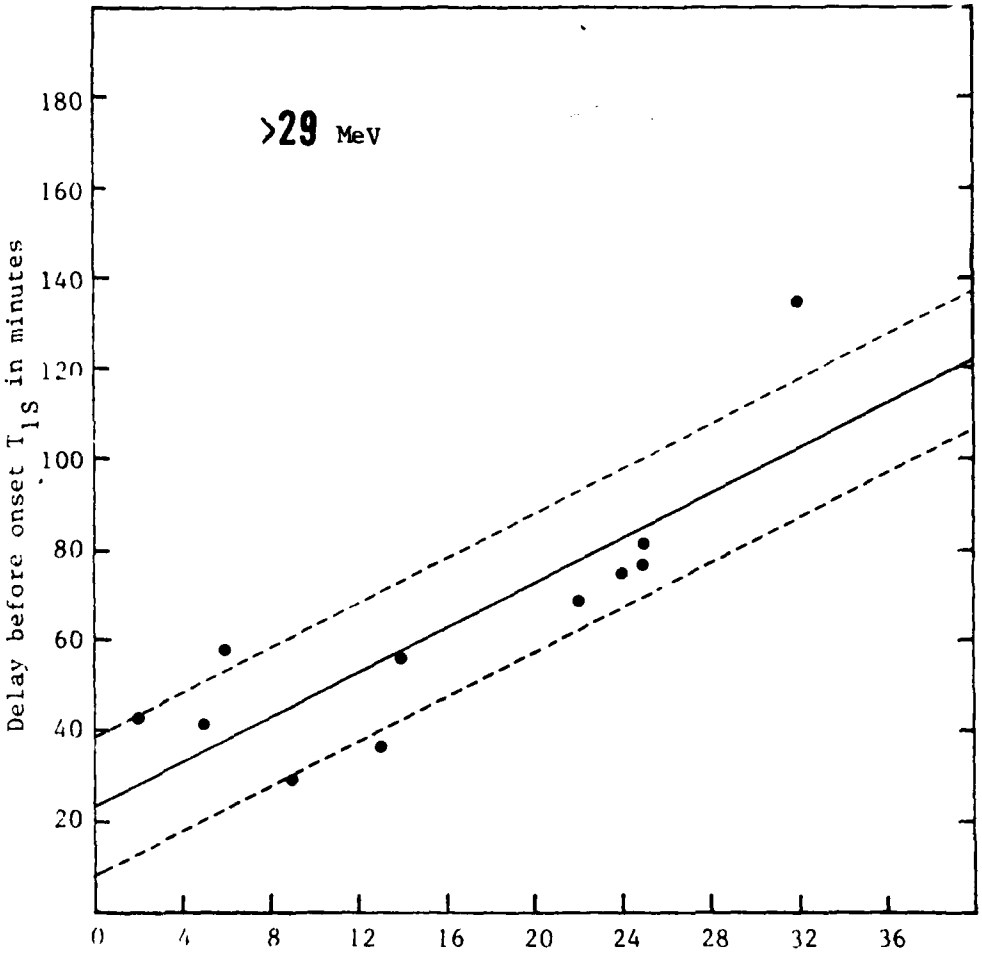
>29 MeV
Delay before onset T_{1S} in minutes
180
160
140
120
100
80
60
40
20
0
4
8
12
16
20
24
28
32
36
Rise Time ρ (H_α) in minutes

Figure 1

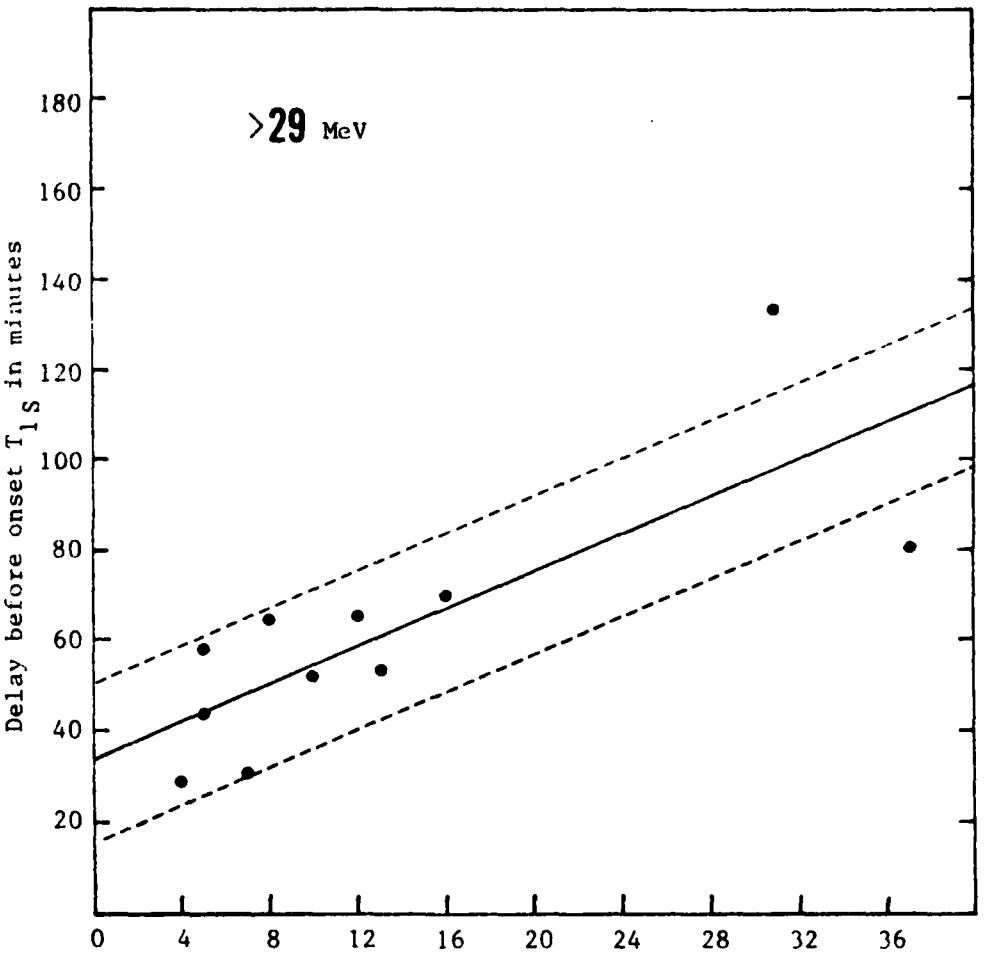
>29 MeV
Delay before onset T_{1S} in minutes
180
160
140
120
100
80
60
40
20
0
4
8
12
16
20
24
28
32
36
Rise Time ρ (2-3 GHz) in minutes

Figure 2

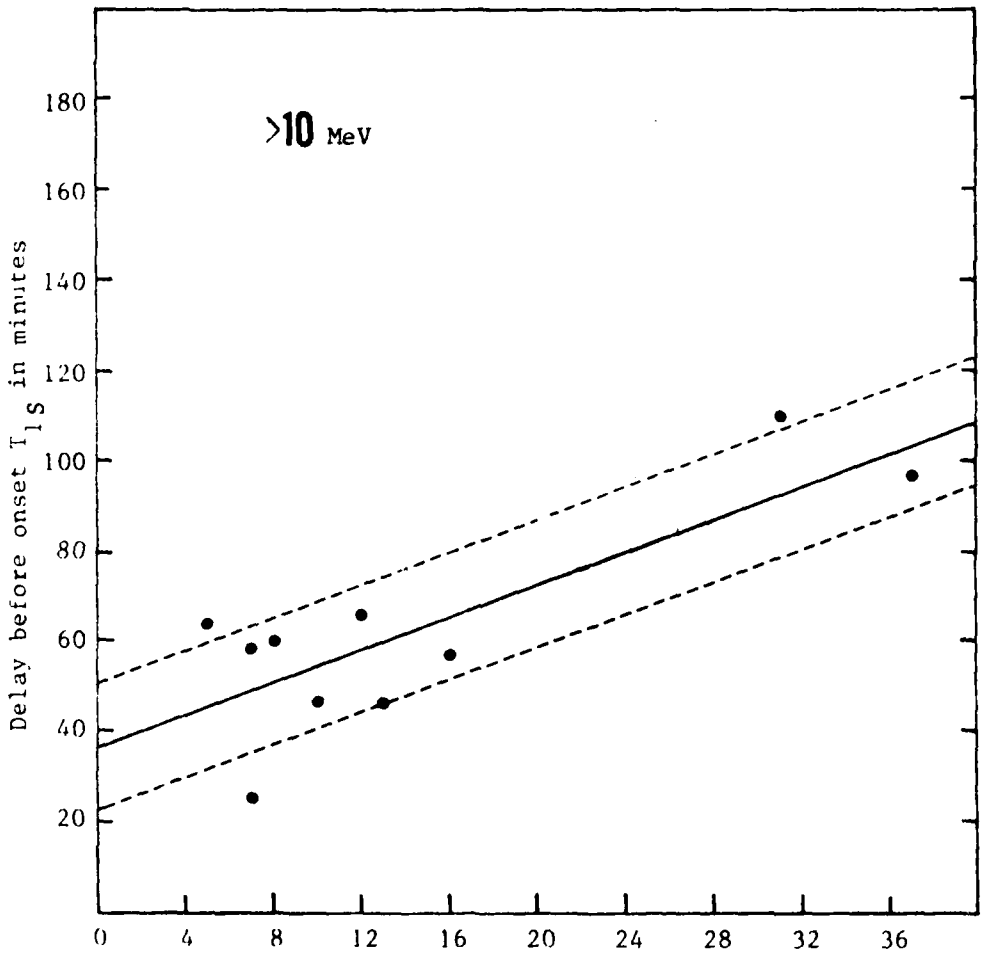

Rise Time ρ (H_α) in minutes

Figure 3

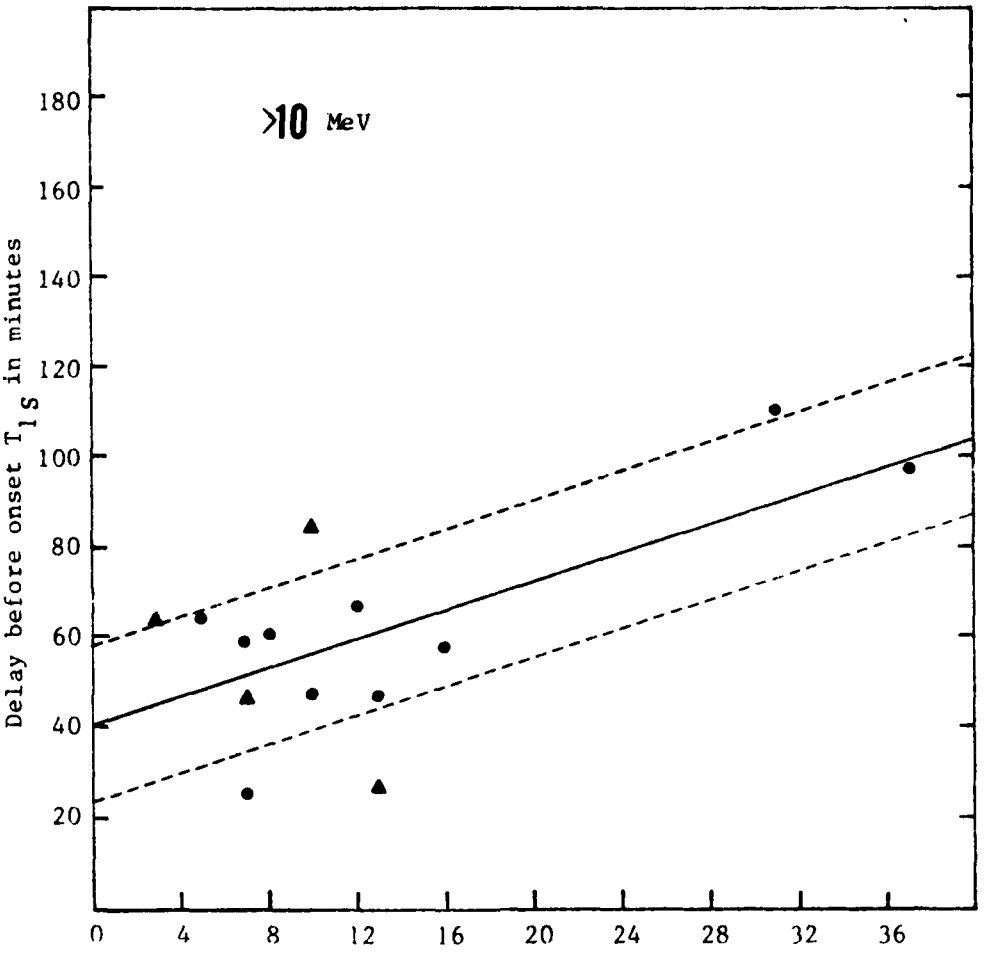
>10 MeV
Delay before onset T_1 S in minutes
180
160
140
120
100
80
60
40
20
0
4
8
12
16
20
24
28
32
36
Rise Time ρ (2-3 GHz) in minutes

Figure 4

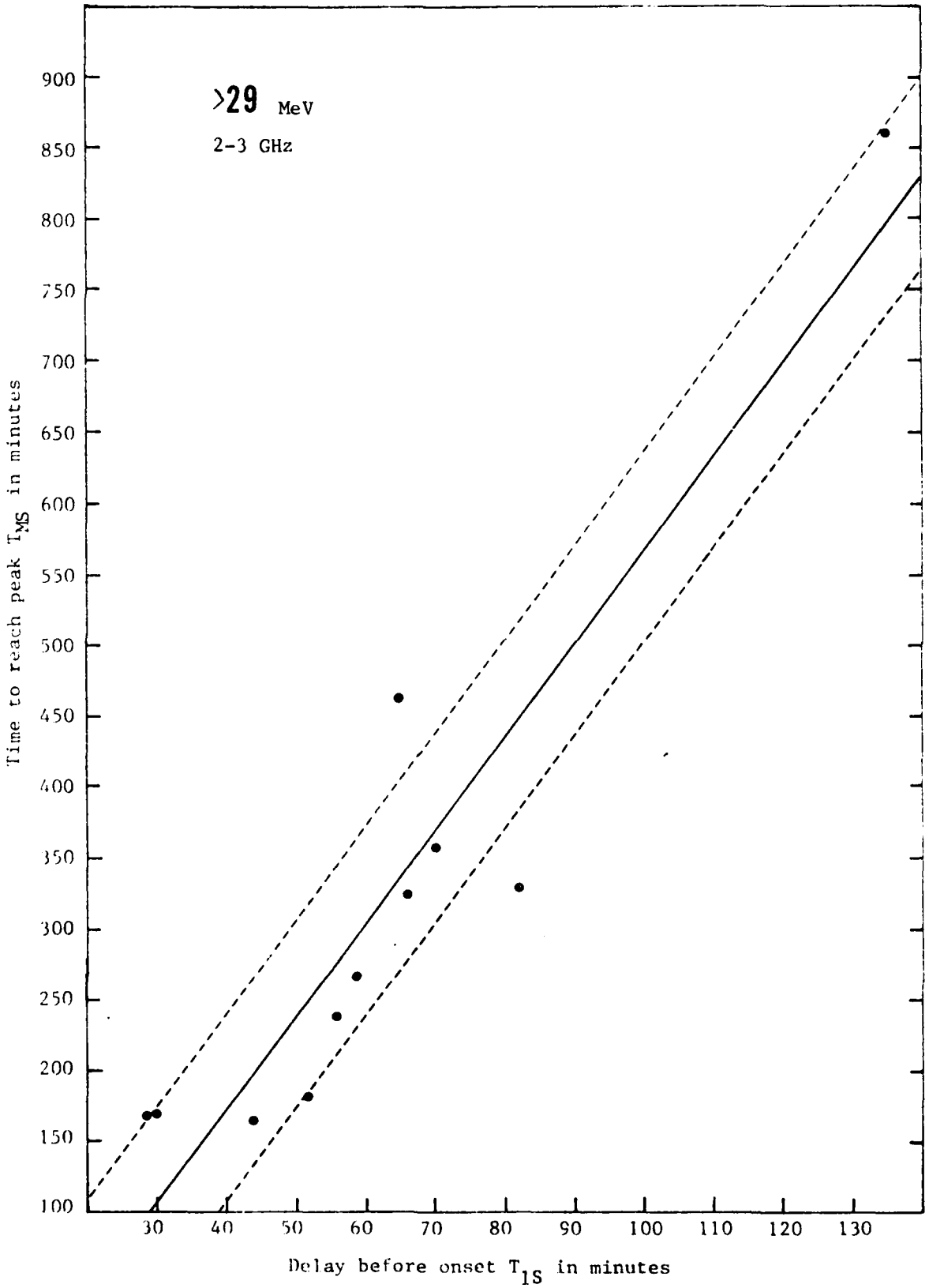
>29 MeV
2-3 GHz
900
850
800
750
700
650
600
550
500
450
400
350
300
250
200
150
100
Time to reach peak T_{MS} in minutes
30
40
50
60
70
80
90
100
110
120
130
Delay before onset T_{1S} in minutes

Figure 5

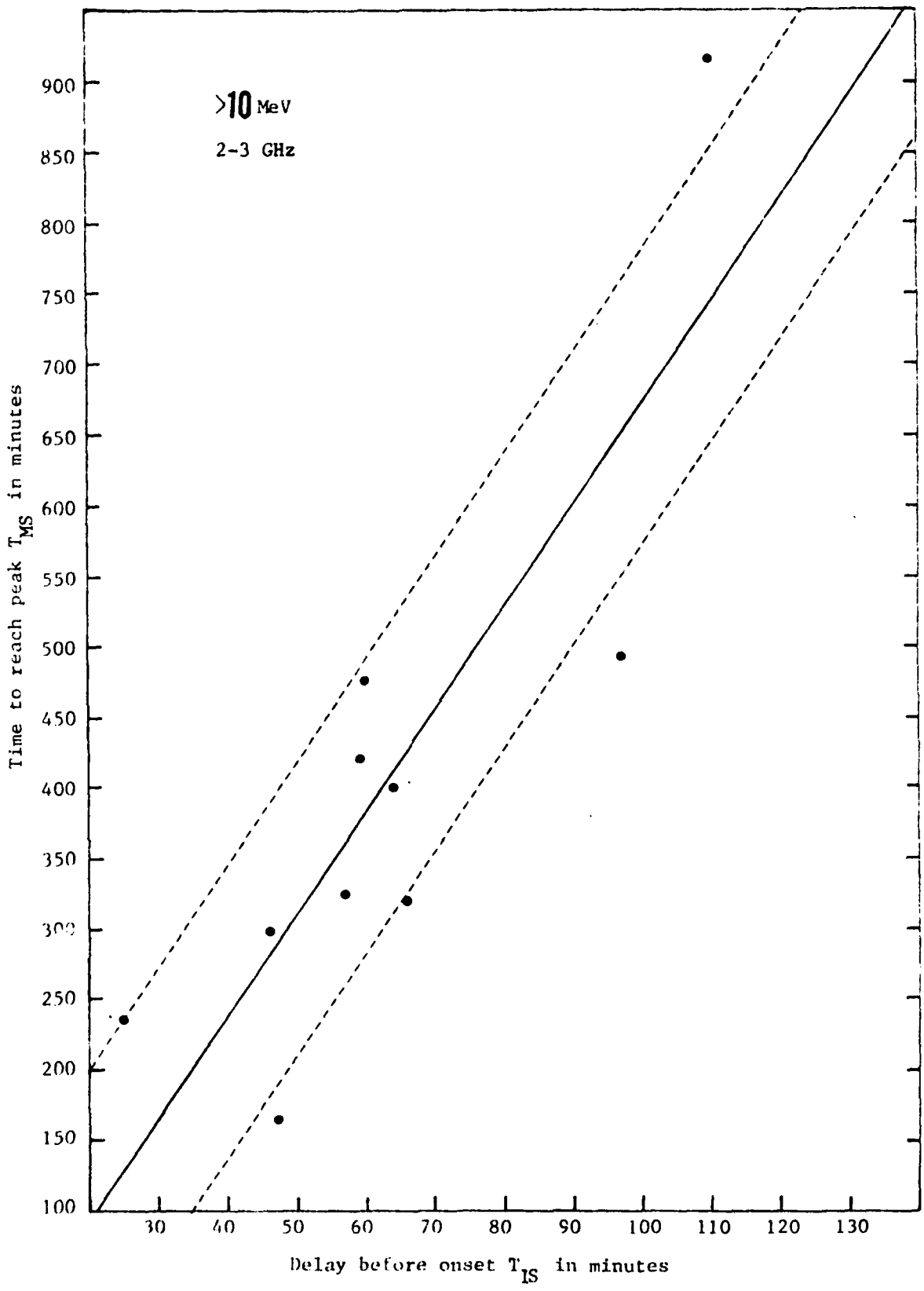
>10 MeV
2-3 GHz
Time to reach peak T_{MS} in minutes
Delay before onset T_{IS} in minutes
900
850
800
750
700
650
600
550
500
450
400
350
300
250
200
150
100
30
40
50
60
70
80
90
100
110
120
130

Figure 6

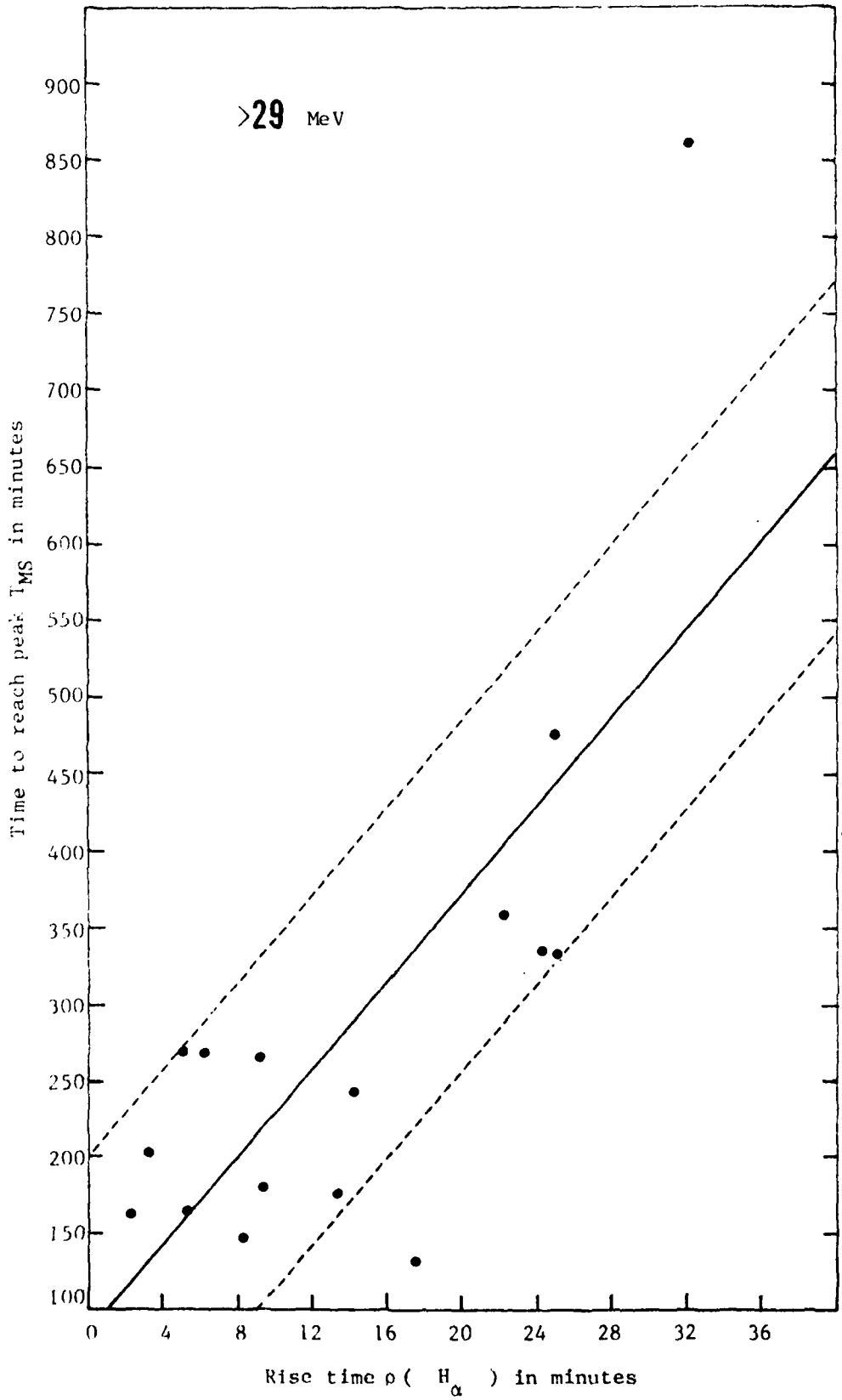
>29 MeV
Time to reach peak T_{MS} in minutes
900
850
800
750
700
650
600
550
500
450
400
350
300
250
200
150
100
0
4
8
12
16
20
24
28
32
36
Rise time ρ(H_α) in minutes

Figure 7

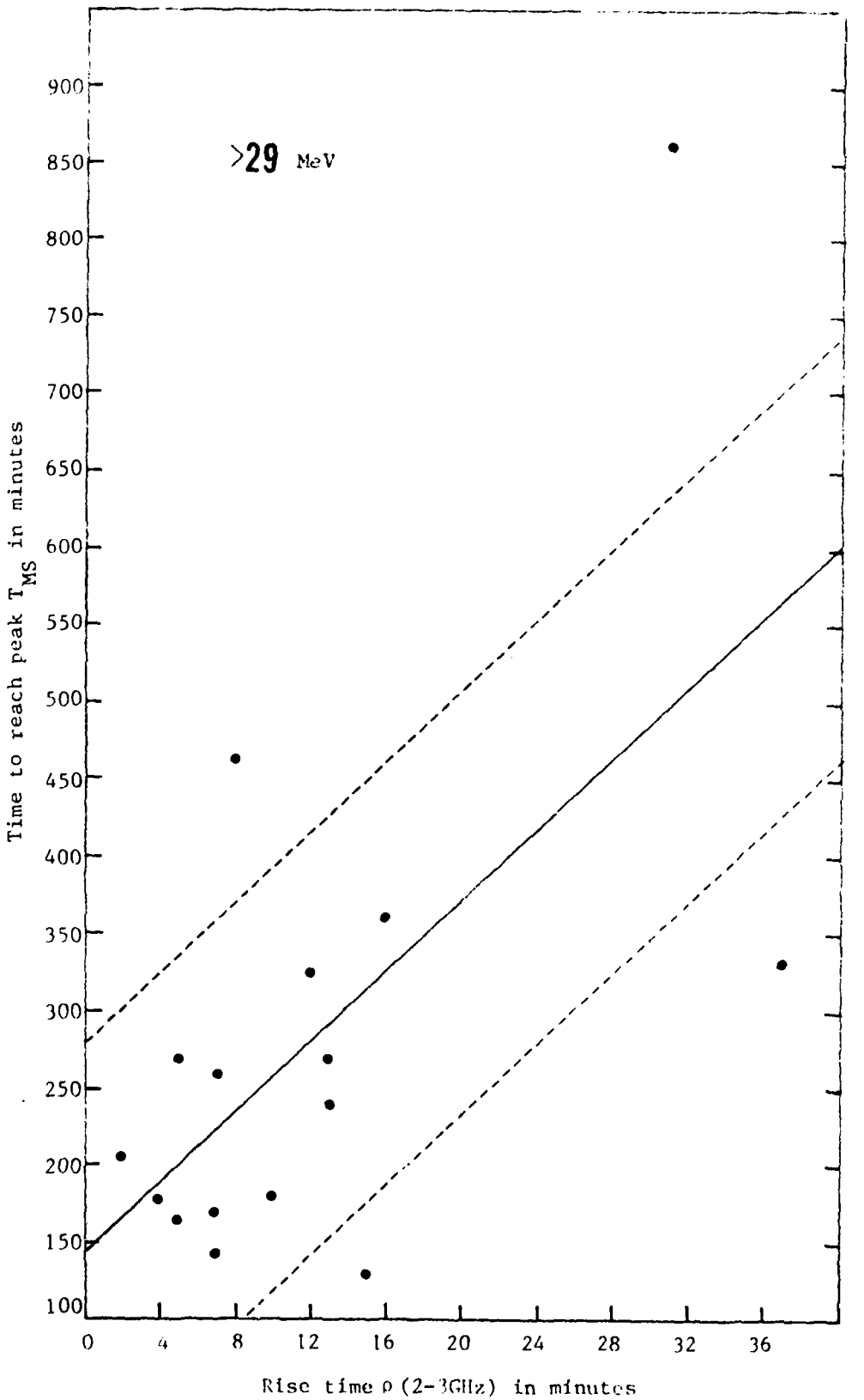
>29 MeV
900
850
800
750
700
650
600
550
500
450
400
350
300
250
200
150
100
0
4
8
12
16
20
24
28
32
36
Time to reach peak T_{MS} in minutes
Rise time ρ (2-3GHz) in minutes

Figure 8

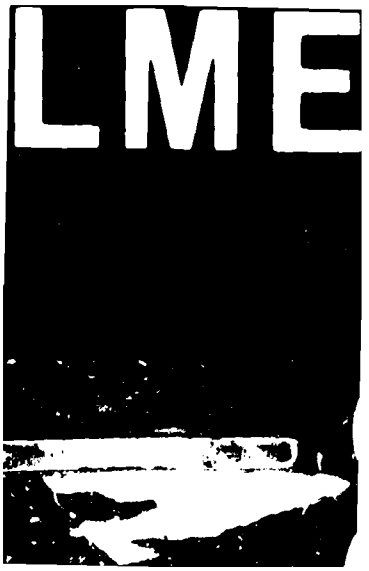
LME